

Technical paper

Selection of manufacturing processes using graph neural networks



Marco Hussong ^{a,*} , Patrick Ruediger-Flore ^a , Matthias Klar ^a , Marius Kloft ^b , Jan C. Aurich ^a

^a Institute for Manufacturing Technology and Production Systems, RPTU Kaiserslautern, Germany

^b Machine Learning Group, RPTU Kaiserslautern, Germany

ARTICLE INFO

Keywords:

Manufacturing process selection
Deep learning
Graph neural network
Process planning

ABSTRACT

The increasing complexity of modern manufacturing, driven by trends such as product customization and shorter product life cycles, presents significant challenges in process planning. Traditional methods for selecting manufacturing processes in industry rely on expert knowledge and manual intervention, which can be time-consuming and error-prone. Systems that can automate the selection of manufacturing processes become increasingly important. Current approaches for the selection of manufacturing processes focus on deep learning that convert the 3D CAD models to intermediate representations such as voxels, point clouds or dexels. However, this transformation can result in the loss of topological, geometrical, or Product and Manufacturing Information (PMI). To address these challenges, this paper proposes a neural network architecture MaProNet. MaProNet is a graph attention neural network (GAT) designed to capture topological and geometrical information through the analysis of Attributed Adjacency Graphs (AAG) and Mesh structures. MaProNet also incorporates a wide range of PMI information.

1. Introduction

Process planning forms the transition between the development and production of a product and involves the selection of all manufacturing processes to ensure a gradual transformation from the raw state to the finished state [1]. Current trends in the manufacturing industry, such as customized products and shorter product life cycles, are increasing the complexity of process planning [2]. In this context, computer-aided process planning systems (CAPP) are becoming increasingly important in assisting with the creation of manufacturing instructions, enabling a continuous integration between computer-aided design (CAD) and computer-aided manufacturing (CAM) and therefore increasing efficiency.

In this context, the selection of manufacturing processes as part of process planning is of central importance, significantly impacting both product quality and costs. Manufacturing process selection demands a deep understanding of the capabilities of the processes, such as the ability to change the shape, material properties or quality of parts. Additionally, it is essential to continuously adapt and learn from any enhancements or changes in the capabilities of manufacturing processes and the machines that execute them [3]. In industry, this is often critical knowledge of process planners, typically gained through experience. However, the selection of manufacturing processes in industry relies on

expert knowledge which requires manual interventions that can be time-consuming and error-prone. Deep learning methods offer great potential for learning how to select manufacturing processes from past data. Due to the effectiveness in handling nonlinearities and discontinuities within the data's feature space, deep learning algorithms can analyze the capability of a manufacturing process in producing various shapes and achieving the required part quality for different materials [4]. Current deep learning approaches, that directly select the manufacturing process, convert the 3D CAD models to intermediate representations such as voxels, Mesh or dexels [5]. This conversion can lead to a loss of PMI, topological or geometrical information. Therefore, this paper proposes a neural network architecture MaProNet. MaProNet is a GAT designed to capture topological and geometrical information through the analysis of AAG and Mesh structures. MaProNet also incorporates a wide range of PMI.

The paper is structured as follows. Section 2 covers a literature review of the relevant works. Section 3 presents the methodology, outlining the framework to train the model and giving a detailed description of the network structure. In Section 4, several studies are conducted ranging from a parameter study, ablation study, performance comparison and test on industrial data. Section 5 presents a summary and outlook.

* Correspondence to: P.O. Box 3049, Kaiserslautern 67653, Germany.

E-mail address: marco.hussong@rptu.de (M. Hussong).

2. Related Works

The evolution of systems to select manufacturing processes has seen considerable advancement through the integration of diverse computational techniques. Existing approaches can be categorized into algorithmic, rule based and ontology systems, and approaches that focus on the use of artificial neural networks (ANN) and deep neural networks (DNN). The approaches using DNN can be further divided into indirect techniques, which select manufacturing processes based on the result of a feature recognition system, and direct techniques, which select the manufacturing processes based on a representation of the 3D CAD model.

In algorithmic, rule and ontology based approaches, predefined rules and algorithms are utilized to determine the most suitable manufacturing processes. Gu and Zhang describe a rule-based process planning system that employs predefined rules to generate manufacturing sequences based on part design requirements, manufacturing capabilities, and operational constraints [6]. Eum et al. introduced an ontology-based modeling approach for manufacturing process selection. This method employs ontologies to represent the relationships between disparate machining features and processes, thereby facilitating the automatic selection of machining operations based on a set of predefined rules and relationships [7]. Deja and Siermiakowski focus on the feature-based generation of machining process plans. The authors propose an algorithmic approach based on feature precedence relationships, process capabilities, and fixturing constraints to determine the selection of manufacturing processes and the sequence of operations [8]. Zhu et al. focus on the development of an automatic manufacturing process selection system based on 3D CAD models. The system automates the analysis of 3D CAD models by recognizing manufacturing features based on geometric shapes and selecting appropriate manufacturing process methods, cutting tools, and machining sequences. It automatically extracts manufacturing features from STL models and offers decisions on manufacturing methods, such as pocketing, drilling, and contouring [9]. Sormaz et al. introduce a rule based tool developed for CAPP with a focus on milling operations. The tool utilizes rules to translate geometric dimensioning and tolerancing requirements into detailed process plans, ensuring the selection of manufacturing processes, tools, and machines [10]. Sormaz and Sarkar propose a semantically integrated manufacturing planning model, an upper-level ontology designed for manufacturing process planning. The ontology addresses three fundamental constraints in process planning: variety, time, and aggregation. It provides a framework to link product features with manufacturing processes, machines, and tools while capturing the temporal and resource dependencies required for dynamic and flexible planning [11]. Furthermore, Sarkar and Sormaz present an ontology model for representing the capabilities of manufacturing resources at the process level. The model integrates the concept of process boundaries, defined by measurable indices such as process capability, and derives its formal structure from the Basic Formal Ontology. By incorporating semantic web technologies and Web Ontology Language axioms, the ontology enables the integration of diverse manufacturing knowledge and supports resource interoperability [12].

Algorithmic and rule based approaches show the following limitations:

- (1) Rule based and algorithmic systems function well within the confines of their defined rules but can be inflexible when faced with scenarios not explicitly accounted for in the rule set.
- (2) Ontology and rule based approaches are limited by the fact that they must be generated and filled manually, making the process labor-intensive and time-consuming.
- (3) Maintaining and updating rule sets can be labor intensive, especially when the underlying knowledge of the system is complex or dynamic. Changes in the capabilities of manufacturing processes or new technologies require manual revision of the rules.

- (4) As the complexity of the system increases with each added rule, rule based systems can be difficult to scale. More rules can lead to higher susceptibility to errors and slower processing.

Rather than following predetermined rules, ANN and DNN models identify patterns and relationships within the data, making them more flexible in responding to new and unforeseen scenarios. Therefore, other approaches focus on the use of ANN to determine manufacturing processes. Ahmad and Haque were among the pioneers in employing ANN for manufacturing process selection in cylindrical surface machining. They employed a feed-forward ANN to categorize cylindrical part features with attributes and ascertain the requisite manufacturing processes and their sequences [13]. Similarly, Yahia et al. developed an intelligent system that integrated ANN with CAD to automate the sequence of manufacturing processes based on component features, thereby demonstrating the flexibility and adaptability of ANN in handling new and complex component types [14]. The paper by Deb et al. introduces a back-propagation ANN for automating the selection of manufacturing operations. The ANN is pre-structured with domain knowledge in the form of thumb rules, which reduces the complexity of the learning process [15]. Rani et al. focus on turn-mill processes and the application of intelligent manufacturing operations selection using STEP. The selection of operations is modeled by a two-layer multi-layer perceptron that categorizes different milling and turning operations based on the inputs of feature type, dimension ratio, feature thread, tolerance, and surface finish [16]. Abdulghafour and Neama develop a two-module system aiming at improving process planning in manufacturing. The first module is responsible for selecting the appropriate manufacturing operation sequence based on attributes like dimension, tolerances, and surface finish. The second module selects the cutting tools based on the machining operations identified by the first module considering factors such as tool type and feature dimensions [17]. Natarajan and Gokulachandran further explored the application of ANN in selecting and sequencing manufacturing operations for prismatic components, demonstrating the efficiency of the Levenberg-Marquardt algorithm in reducing error rates and enhancing the precision of process planning [18]. The ANN approaches have the following limitations:

- (1) ANN approaches do not consider the direct shape of the 3D CAD model, instead, the shape is modeled through different types of features (e.g. hole) and parametric descriptions of the feature type (e.g. diameter and depth) that are used as inputs for the ANN
- (2) Through the inability for direct shape analysis, the ANN approaches highly depend on a feature recognition method. Errors in the feature recognition model will consequently lead to errors in the selection of manufacturing processes.
- (3) Furthermore, the predictions of the ANN are based on individual features. The interaction of features and the overall part structure is not considered.

Therefore, subsequent methodologies employ DNN to predict manufacturing processes based on feature recognition approaches. Wang et al. propose a machining feature process route planning method utilizing graph convolutional neural networks (CNN). This method addresses the limitation of existing approaches that focus only on individual features and neglect the overall part structure. By employing attribute graphs where nodes represent machining features and edges capture their interactions, the authors develop a model that predicts manufacturing processes [19]. The paper focuses mainly on the prediction of milling and drilling technologies and does not consider rotational parts that require turning as a manufacturing technology. Zhao et al. propose an integrated framework that utilizes deep learning and sequence mining for manufacturing process and sequence selection. The method identifies manufacturing features from 3D part designs using a GNN and predicts necessary processes with a CNN, considering factors such as shape, material, and quality [20]. The predictions of the two

DNN in Zhao et al. are interdependent. Therefore, errors in the initial stage of feature recognition propagate and cause further inaccuracies in the subsequent stage of selecting the appropriate manufacturing processes.

The aforementioned methodologies illustrate the diversity of scientific approaches that leverage the relationship between features and manufacturing processes. Therefore, the following works consider feature recognition techniques. The literature on feature recognition is extensive, therefore this paper focuses specifically on recent efforts that employ deep learning methods for feature recognition. Alternative methods for feature recognition are detailed for example in Shi et al. [21].

Zhang et al. present FeatureNet, a framework using 3D CNN for machining feature recognition from 3D CAD models. The system is trained on a large-scale dataset that applies a single feature to a basic cuboid shape. The network recognizes features from voxelized models [22]. Ma et al. propose a CNN for automatic recognition of machining features from 3D point cloud data. The method uses a modified PointNet architecture to classify 24 types of machining features by training on a large sample set of point cloud data generated from 3D CAD models [23]. Shi et al. present a method using multiple sectional view representation for recognizing machining features in 3D CAD models [24]. Ning et al. propose a machining feature recognition method based on a 3D CNN combined with a graph based method. The approach combines the graph based method for identifying individual features that are then classified based on a 3D CNN [25]. Yeo et al. propose a machining feature recognition method that integrates directly with 3D CAD systems. The method uses feature descriptors, such as face type, curvature of face or normal vector, generated from boundary representation (B-Rep) models by integer encoding, allowing for feature recognition without converting models to voxel or point cloud formats [26]. Colligan et al. present Hierarchical CADNet, a hierarchical graph CNN designed for machining feature recognition. The method uses a hierarchical B-Rep graph structure that encodes both the geometry and topology of 3D CAD models [27]. Lee et al. propose a 3D CNN for machining feature recognition from 3D CAD models. The method integrates gradient-weighted class activation mapping (Grad-CAM) to provide visual explanations for the recognized features, aiming to identify and localize machining features from voxel representations of 3D CAD models [28]. Yao et al. propose a machining feature recognition approach based on a hierarchical DNN to identify multiple features in point cloud models. The method utilizes PointNet++ for single feature recognition and introduces a feature segmentation technique to separate complex multi-feature models into single feature models for classification [29]. Zhang et al. propose a machining feature recognition method based on a multi-task DNN, called Associatively Segmenting and Identifying Network (ASIN). This method performs three tasks: machining feature segmentation, feature identification, and bottom face identification using point cloud data from 3D CAD models [30]. Jia et al. propose a machining feature recognition method based on an improved Mesh DNN model. This approach combines an improved version of MeshCNN with Faster RCNN for feature extraction and classification [31]. Lee et al. propose BRepGAT, a graph based attention DNN designed to segment machining feature faces from B-Rep models. The method uses GAT to process graph data derived from 3D CAD models, focusing on propagating information from nodes to improve machining feature recognition accuracy [32]. Wang et al. propose a hybrid learning framework for manufacturing feature recognition based on GNN. The framework integrates rule based methods with graph based learning to recognize interacting features from CAD models by decomposing them into isolated features for classification [33]. Wu et al. propose a semi-supervised learning framework for machining feature recognition, designed to address the challenges of limited labeled datasets. The framework uses self-supervised learning to extract representations from large unlabeled data and incorporates lightweight techniques to create more efficient models, specifically FeatureNetLite and MsvNetLite [34].

Zhang et al. propose BrepMFR, a DNN designed to enhance machining feature recognition in B-Rep models. The method employs a GNN based on a Transformer architecture and incorporates domain adaptation techniques to improve the generalization of synthetic training data to real-world 3D CAD models [35]. Wu et al. propose a GNN for multi-task machining feature recognition. The method uses an AAG representation to capture the topological, geometric, and extended attributes from B-Rep models. The network is designed to perform semantic segmentation, instance segmentation, and bottom face segmentation simultaneously [36]. The limitations of feature recognition methods are:

- (1) Complex and intersecting features are still hard to recognize
- (2) Features need to be defined for all possible geometrical shapes of a part, therefore, defining a closed set of features is difficult since new features can appear that were never seen before,
- (3) The definition of the relationship between features and manufacturing process can be ambiguous, therefore defining a suitable manufacturing process for a feature is not always trivial. Certain features can be produced by several manufacturing processes.

Therefore, subsequent methodologies employ DNN to directly select manufacturing processes, without the need to determine features. The objective of these approaches is for the DNN model to learn to recognize the spatial metadata that constitutes a feature, rather than directly identifying the feature as a geometrical entity itself, thereby mitigating the previously mentioned challenges in feature recognition. Peddireddy et al. present a manufacturing process identification system that leverages 3D CNN and transfer learning to classify the manufacturing processes of milling and turning from voxelized 3D CAD models. The proposed system utilizes a large-scale dataset of synthesized workpiece models to train the DNN [37]. The paper by Fu et al. focuses on the development of an improved dixel representation for use in CNN applied to 3D CAD models. The approach provides a 3D geometry descriptor that captures the position, size, and surface information of a 3D CAD model with high resolution, enabling better recognition of small-scale shapes [38]. The paper by Wang and Rosen focuses on manufacturing process classification using Heat Kernel Signature and CNN. To improve the prediction accuracy, they developed a DNN approach that utilizes Heat Kernel Signature to describe the geometry of parts, derived from triangle Mesh representations [39]. The paper by Yan et al. presents a process-aware part retrieval method using unsupervised deep learning. The authors developed an autoencoder that uses both part shape and material properties to generate a latent vector representation [40]. Yan and Melkote introduce an automated manufacturability analysis and manufacturing process selection method using a combination of DNN. The proposed system uses an deep generative model based on an autoencoder to represent manufacturing operations and combines them with a Siamese Neural Network to compare part shapes and evaluate manufacturability [41]. Yan et al. propose a semantic segmentation method for machinable volume decomposition based on DNN. The approach utilizes generative pre-trained process capability models to identify machinable volumes and assign candidate manufacturing processes to each voxel in a 3D CAD model [42]. Another study by Wang et al. compares various shape descriptors and includes material properties for part similarity searches aimed at automating the selection of manufacturing processes [5]. The limitation of the proposed approaches is that they focus mainly on the shape transformation capabilities of manufacturing technologies, but do not consider PMI. Yan et al. and Wang et al. incorporate material properties but neglect other information such as surface requirements or other tolerances.

Zhao and Melkote focus on learning the manufacturing capabilities of machining and finishing processes using a DNN. The proposed model integrates a 3D CNN with a multi-layer perceptron (MLP) to predict manufacturing process labels based on a voxelized part geometry, material properties, and part quality [4]. This approach is limited in the

scope of features that are considered and that the prediction of the network is based on a single feature that defines the part. Furthermore, PMI is considered on a global level. Therefore, several PMI definitions in the 3D CAD model require an aggregation to a global score, hindering the local interpretation of PMI through DNN. Additionally, the approach by Zhao and Melkote uses voxelized 3D CAD models as input. Voxelized models either require large computational effort when high resolution is chosen or can not adequately capture small geometrical shapes with low resolutions.

Therefore, this paper proposes a neural network architecture MaProNet, specifically tailored for the selection of manufacturing processes. MaProNet is a GAT, that leverages the geometric and topological properties of faces in the 3D CAD model, analyzing the shape of different faces through Meshes and AAG. PMI is also incorporated into the structure, enabling a sophisticated interpretation of manufacturing technologies without the need for feature recognition. The architecture of MaProNet incorporates a GAT structure as the attention mechanism provides a significant advantage by enabling the model to dynamically adjust its focus based on the relative importance of the input components, such as the AAG and Mesh. This facilitates a more refined representation of both the AAG and Mesh, leading to improved accuracy

and robustness in the model's predictions.

Due to the definition of MaProNet, this paper extends the prediction of manufacturing processes to a semantic segmentation task on graphs. The objective of semantic segmentation in this context is to assign each face (node of the graph) to a specific category, represented by the different manufacturing processes. This enables a precise analysis of chosen manufacturing technologies for different faces of the 3D CAD model increasing the interpretability of the results.

To optimize the network structure, a parameter study is conducted in which the embedding size, number of attention heads and the number of layers are varied. The performance is evaluated using different measures such as Accuracy, F1-Score and Intersection over Union.

Requiring semantic labels for the 3D CAD models for the prediction of MaProNet, this paper also describes the creation of a new dataset for manufacturing process selection. The dataset combines a large amount of geometrical features and PMI in different 3D CAD models.

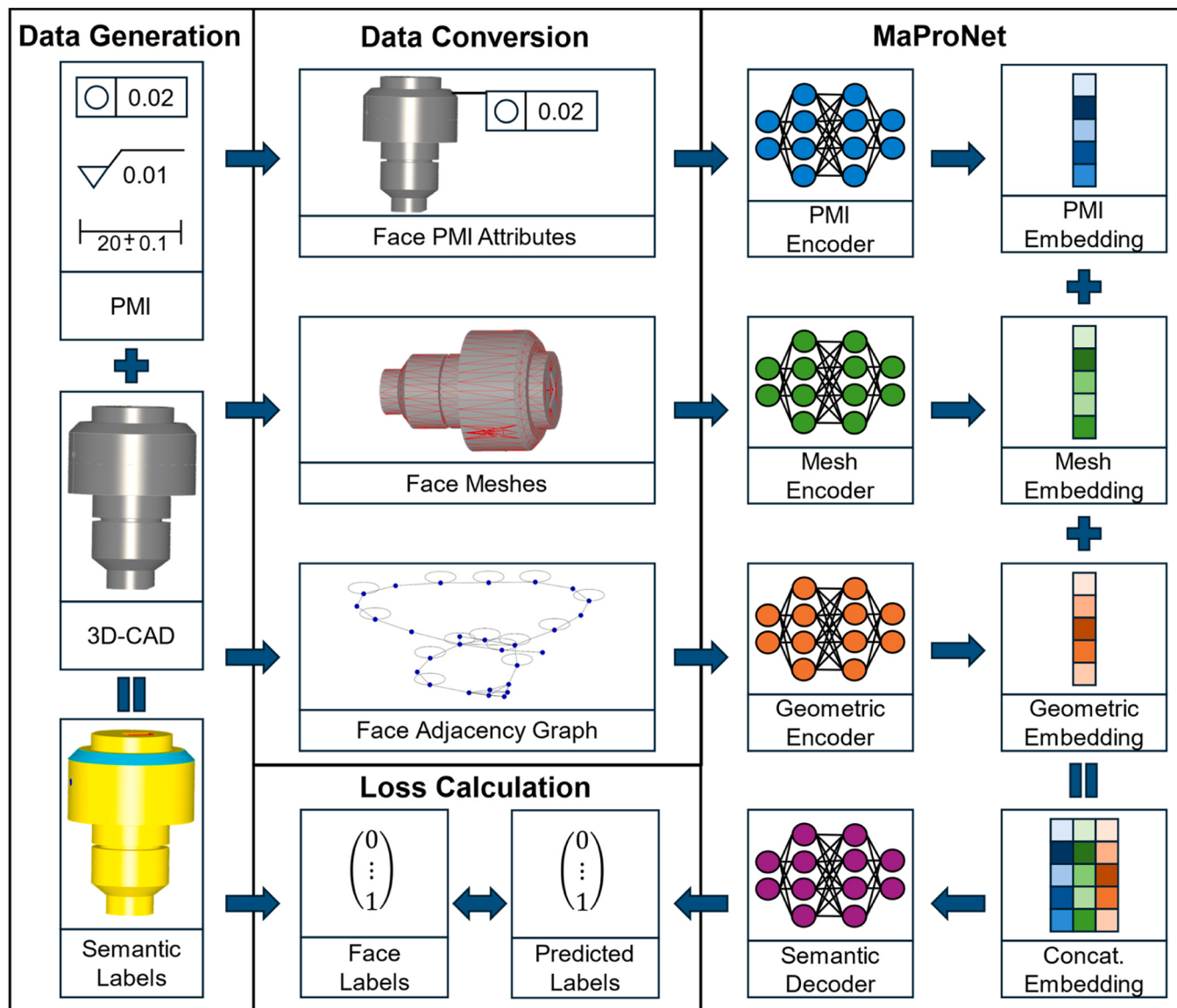


Fig. 1. Illustration of the proposed framework.

3. Methodology

3.1. Overview of the framework

Building on recent advancements in DNN approaches for the selection of manufacturing processes, this paper proposes a GAT-based framework for the semantic segmentation of 3D CAD models. Semantic segmentation provides a face-level detail, allowing for a more precise understanding of the 3D CAD model's content rather than just identifying the overall object class. The advantage of using a graph representation of 3D CAD models is that graphs can effectively capture the geometrical and topological relationships between different faces of the model, which is challenging to achieve with point clouds or voxel grids. The 3D models in the BRep format are converted to Mesh graphs and AAG, while the PMI data is calculated in class settings, to serve as the input for MaProNet. The inputs are used in three different encoder heads of the network, that create an embedding of the different information types. The different embeddings are processed by a decoder that converts the embeddings into a multi-class classification on a face level (semantic segmentation). The objective is to assign each face of the 3D model to a specific category, represented by the different manufacturing processes. Within the framework, the data for the training of the network is created synthetically using the programming language Python and different packages such as cadquery and pythonocc. The data generation includes the creation of 60,000 3D CAD models with PMI information and the corresponding semantic labels. Fig. 1 summarizes the pipeline of the framework.

3.2. Generation of dataset for the selection of manufacturing processes

The preparation of training datasets for deep learning poses a significant challenge. Datasets with industrial 3D CAD models for semantic segmentation typically require a large annotation effort, since every face of the 3D CAD model must be classified. Therefore, industrial datasets for the selection of manufacturing processes for semantic segmentation are not publicly available, but the performance of data-driven models depends on large-scale training data. Therefore, a synthetically created dataset has to be designed for the selection of manufacturing processes on a face level. Zhao et al. introduced the first dataset for the selection of manufacturing processes modeled as a classification task [4], where a single machining feature is applied to a basic geometrical shape.

The dataset generation approach presented in this paper is based on the concepts introduced by Zhao et al. [4], with several extensions and enhancements. For PMI, in addition to surface finishes and size tolerances, this dataset also includes descriptions of geometric tolerances, such as flatness, straightness, circularity, and roundness. Moreover, the labels of the manufacturing processes are not modeled globally (for the whole 3D-CAD model) as in Zhao et al. [4], but on a local level for the semantic segmentation. With that extension, this approach is able to consider parts, where more than one feature builds the overall shape of the part. Consequently, within the proposed dataset, a defined label indicates the manufacturing processes required, to reach the geometrical and quality requirements for every face of the 3D-CAD model introducing the task of semantic segmentation on the 3D shapes. As manufacturing processes milling, turning, drilling, grinding, and reaming are considered. The manufacturing processes are categorized into roughing and finishing processes. The roughing technologies involve removing a substantial amount of excess material from workpieces and produce the desired 3D part shapes and geometries. Finishing technologies aim to refine the geometries produced by the roughing technologies to comply with restrictions defined by PMI, and do not usually generate the primary part shapes. Therefore, the finishing processes are coupled with a primary shape generation process. As a result, a face of a 3D shape can have one of six labels (turning, milling, drilling, turning and grinding, milling and grinding, drilling and reaming). The models

To model the different shapes of the 3D CAD models, a large set of

machining features is used. The combination of features defines the overall shape of the part. The features are randomly chosen and randomly positioned on different basic shapes. Therefore, different interactions of features can be modeled within the proposed dataset. The features are built upon the basic shapes of a cuboid or a cylinder. A comprehensive overview of all features with their parameters and PMI can be found in the Appendix. The following features were modeled: cuboid and round bosses, through and blind steps/slots, cylinder steps, rectangular and circular end pockets, milled and drilled blind/through holes, counterbore and countersink holes, chamfers, fillets, grooves, belt steps, and tapers. After generating the 3D models, they were validated to ensure both geometrical integrity and topological feasibility. However, the manufacturability of the parts is not considered, as the objective of our model is not to assess the manufacturability of the 3D components. It is assumed that the models provided by the industry for which the model is used are manufacturable or evaluated for manufacturability at an earlier or later stage in the process. Consequently, the aspect of manufacturability is not addressed for the synthetically created data.

The dataset also includes different PMI, such as geometrical and dimensional tolerances or surface requirements. They influence the choice of technologies due to different quality definitions. For example, if a fine-grained surface finish is required, purely using milling technology to create the geometry of the shape will not satisfy the surface restriction requirement, therefore an additional grinding step will be necessary. The PMI is modeled using technology tables. Table 1 shows an exemplary table.

As can be seen, different classes can be derived from the different numerical values. A similar approach is chosen for all the PMI used in this contribution. For example, the dimensional tolerances are converted to international tolerance grades (IT grades) referencing the choice of a specific technology. It is assumed that roughing technologies are able to produce geometries with average application. For the finishing technologies also the less frequent applications are considered, to cover the whole spectrum of possible restrictions for example surface finishes (see Table 1). If two technologies are able to produce the same tolerance value (e.g. for 1.6 µm, both drilling and reaming are feasible options), roughing is preferred over finishing, as roughing processes are typically more efficient and therefore more economical.

The material choice is modeled to influence the relationship between PMI class and the used manufacturing process. Therefore, for constant PMI, depending on the choice of material, finishing processes need to be considered or not. Fig. 2 shows some examples of the dataset. Please note, that the stock faces shown here are just for illustration to clearly distinguish the features, but are not considered in the prediction of MaProNet. Fig. 3 shows an example of a synthetically created 3D CAD model with labels and PMI.

3.3. Architecture of MaProNet

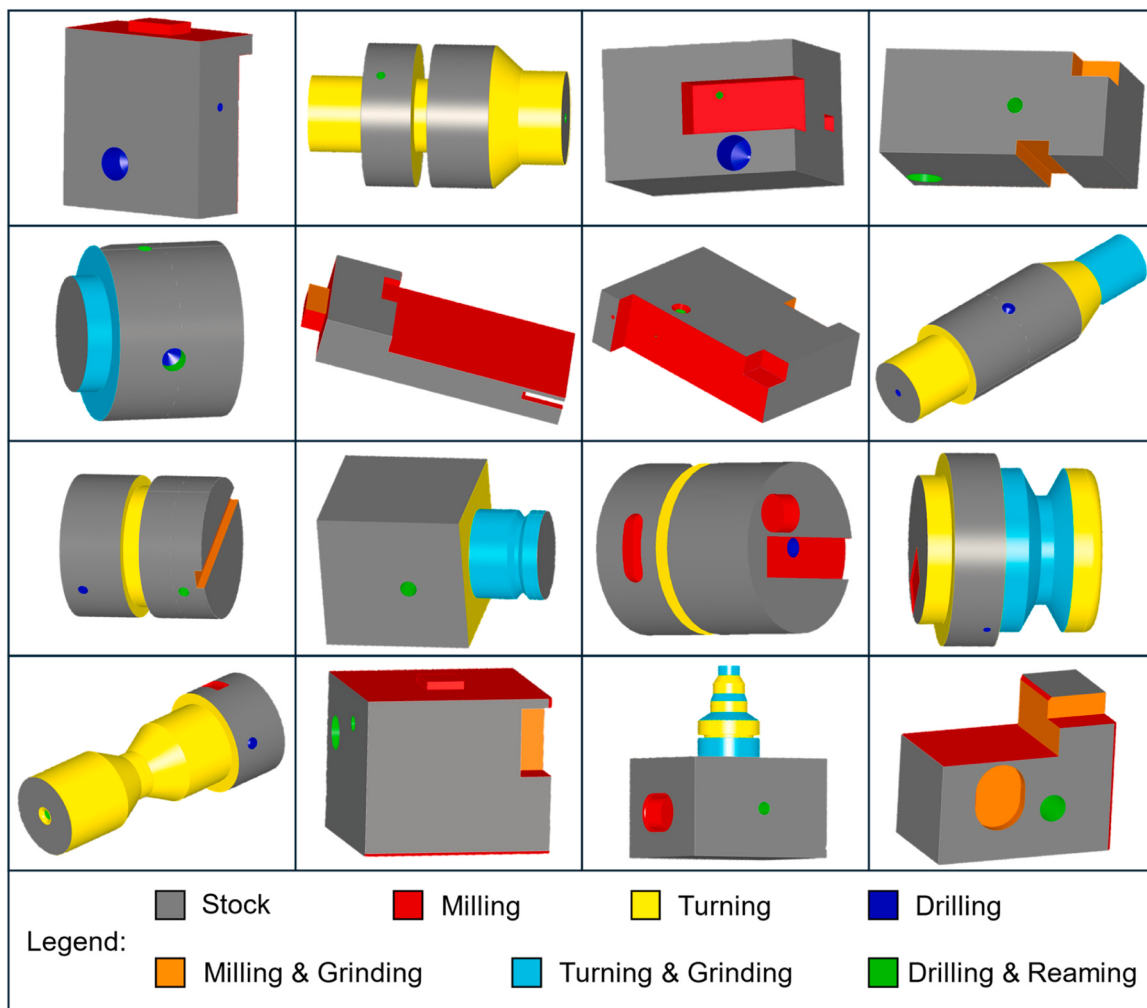
3.3.1. Overall description of MaProNet

Fig. 4 shows the overall structure of MaProNet. As can be seen, the network consists of three input heads, the encoders, and one output head, the decoder. The encoders convert the different input structures PMI, AAG, and Mesh using a defined number (n) of layer blocks to an embedding size (m). Depending on the input, the encoders include different types of layers, such as graph attention, batch normalization, linear, activation and attention pooling. These are closely described in Section 3.4. The parameters that coincide with the number of layer blocks (n) and the embedding size (m) can be chosen when training the model. The size of these are determined by a parameter study in Section 4.1. The different outputs of the encoders, that form the embedding, are concatenated and used as the input for the decoder. The decoder analyses the representation and performs the predictions. The predictions are done locally, therefore predictions are performed for every face of the 3D model.

Table 1

Surface Roughness produced by various machining methods based on ASME B.16-1 [43].

| Machining Operation | Surface Roughness (Micrometers μm) | | | | | | | | |
|---|--|------|-----|-----|-----|-----|-----|-----|-----|
| | 0.025 | 0.05 | 0.1 | 0.2 | 0.4 | 0.8 | 1.6 | 3.2 | 6.3 |
| Milling | | | | | | | | | |
| Turning | | | | | | | | | |
| Drilling | | | | | | | | | |
| Grinding | | | | | | | | | |
| Reaming | | | | | | | | | |
| Legend: | | | | | | | | | |
| ■ Average Application ■ Less Frequent Application | | | | | | | | | |

**Fig. 2.** Examples from the synthetical dataset.

3.3.2. Inputs for the multiple heads

The PMI, AAG and Meshes are used as inputs for the different encoders. For the PMI, the categories are represented by different classes (1–16), which serve as the input. Therefore, the input vector for the PMI is of shape 1×7 with the seven categories of material, dimensional tolerance, surface finish, straightness, flatness, circularity, and

cylindricity. The second input is an AAG. An AAG of a 3D CAD model is a mathematical representation that captures the relationships between neighboring faces of the model and represents them as a graph. This neighboring information supports the network to distinguish between faces that form a coherent set, influenced by the process technology. For instance, when manufacturing a pocket, both the side faces and the

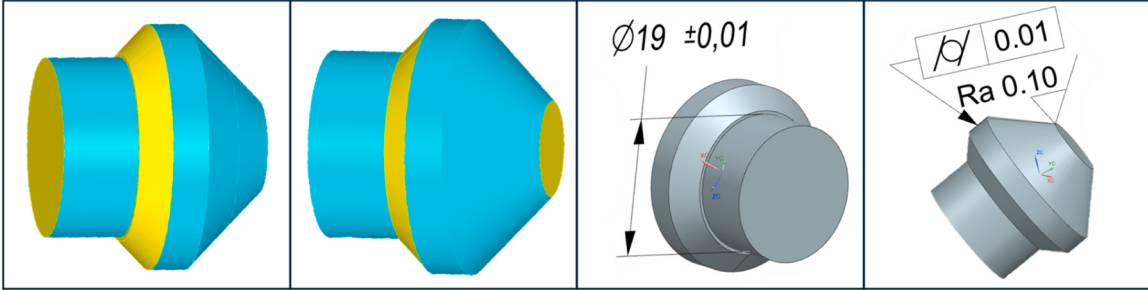


Fig. 3. Full Example with Labels and PMI.

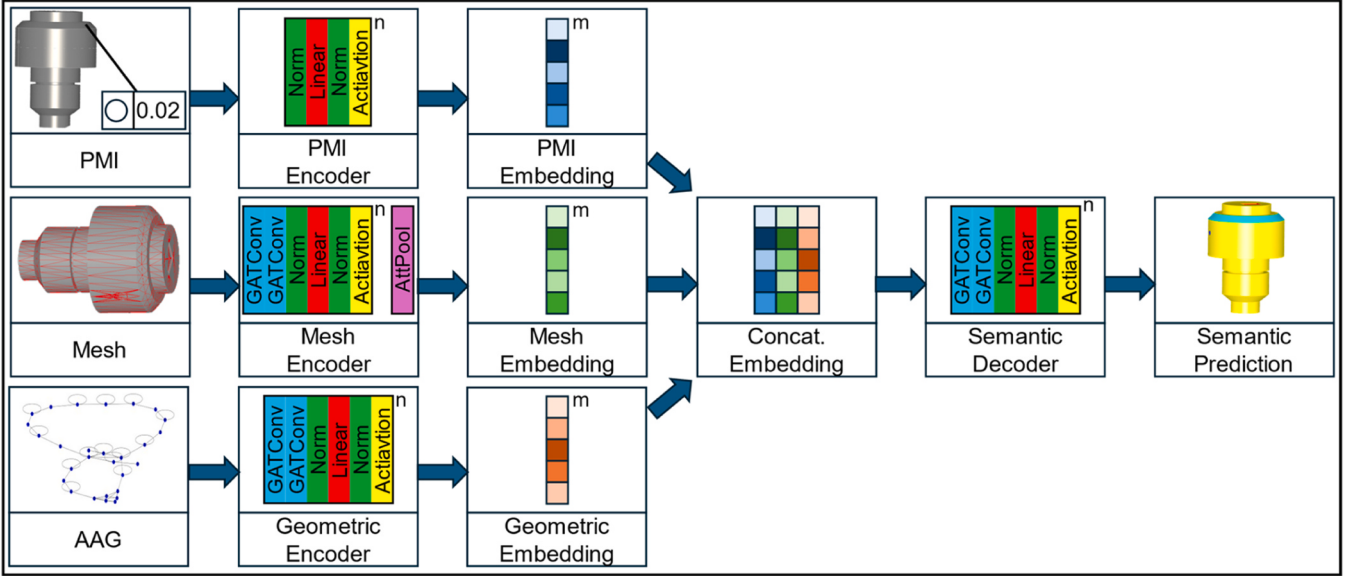


Fig. 4. Architecture of MaProNet.

ground face are affected by the same process, and by incorporating this neighboring information, the network can differentiate between faces that share a common technological relationship.

The nodes respectively edges of the graph represent the faces and the edges that connect the different faces. For AAG different attributes can be defined for each node and edge of the graph, that represent attributes of the faces respectively edges of the 3D CAD model. Table 2 summarizes the implemented attributes for the AAG of this approach.

3.4. Description of encoder, decoder, and corresponding layers

The different heads of MaProNet consist of layer blocks, that can be specified as parameters in the architecture of the model. The embedding size, that is the output of the different input heads, is divided by the number of blocks, therefore, the output of every block is a fraction of the total embedding. The PMI encoder consists effectively of a MLP, with a batch normalization and a linear layer followed by another batch normalization and an activation function. Based on preliminary experiments, the activation function is chosen to be leaky relu. The primary function of the linear layer is to transform its input data into an output space of a desired dimension. This transformation is achieved through a matrix multiplication of the input features and the layer's weights, followed by the addition of a bias term. The AAG encoder consists of two GAT layers, followed by the MLP architecture of the PMI encoder. The GAT layer utilizes a self-attention mechanism to dynamically assign varying levels of importance to different nodes within a neighborhood by computing attention coefficients. These coefficients dictate the

influence that each neighboring node should have over the updated attributes of a given node. This process ensures that more relevant nodes have a greater impact, enhancing the model's ability to focus on significant nodes for the task at hand. These GAT layers also employ multi-head attention. This technique involves multiple independent attention mechanisms that operate simultaneously, providing multiple learned representations for each node. These are then combined, by averaging, which helps stabilize the learning process across different representation subspaces.

The advantage of GAT over other approaches such as Graph Convolution or GraphSAGE lies in the described attention mechanism. This mechanism is particularly beneficial for the selection of manufacturing processes, as it enables the network to prioritize the most influential components of the input data, enhancing both interpretability and predictive performance. One of the inputs in this context is the AAG that encodes the neighboring relationships between faces. The attention mechanism allows the neural network to assign greater importance to specific faces that have a stronger contribution to the selection of the manufacturing process. This adaptive weighting ensures that the model selectively emphasizes the most relevant connections while reducing the influence of less critical ones. A similar argument applies to the Mesh representation. By employing attention, the network can focus on specific regions of the Mesh that are more indicative of the manufacturing process. This capability is particularly important for capturing localized geometric features or structures that are critical for the predictive task.

The Mesh encoder is similarly built compared to the AAG encoder,

Table 2

Attributes used in the AAG representation.

| Entity of Graph / 3D CAD Model | Attribute | Description |
|--------------------------------|-------------------------|--|
| Node / Face | Type | The type of face e. g. plane or cylinder |
| Node / Face | Center belongs to part | Check, if the center of the surface is inside the part, on the surface, or outside the part. |
| Node / Face | Center Coordinates | x, y, z value of the center of mass |
| Node / Face | Normal Vector | x, y, z value of the normal vector in the center |
| Node / Face | Ratio | The ratio between different sides of the face |
| Node / Face | Area | The area of the surface |
| Edge / Connecting Edge | Vexity | Selection if the edge is convex or concave |
| Edge / Connecting Edge | Type | The type of edge e. g. line or circle |
| Edge / Connecting Edge | Closed | Check, if the start and end point is the same |
| Edge / Connecting Edge | Center Coordinates | x, y, z value of the center of mass |
| Edge / Connecting Edge | Tangent Vector | x, y, z value of the tangent vector in the center |
| Edge / Connecting Edge | First Point Coordinates | x, y, z value of the start point of the edge |
| Edge / Connecting Edge | Last Point Coordinates | x, y, z value of the start point of the edge |
| Edge / Connecting Edge | Length | The length of the edge |

The third input is a triangulated Mesh with a linear deflection of 0.1. The attributes of the nodes are the x, y, and z values from the coordinates of a specific point on the face of the 3D CAD model. The Meshes are created for each face of the 3D CAD model. Note that the Mesh input operates on a different level compared to the AAG. The AAG represents the whole structure of the 3D CAD model, whereas one Mesh represents the structure of a specific face of the 3D CAD model.

but in contrast to the AAG encoder, the Mesh encoder operates on a lower graph level. The AAG represents the neighboring relations of the different faces of the 3D CAD model whereas the Mesh represents triangles on the surface of a specific face of the 3D CAD model. Using the described architecture of the Mesh encoder will output a whole graph for the face of the 3D CAD model rather than an embedding of attributes for the face. To reach a structure that corresponds to the embedding of a face the Mesh is pooled using an attentional aggregation layer consisting of a linear layer followed by a sigmoid activation. The decoder consists of the same structure as the AAG encoder.

3.5. Loss function and metrics for the multi-class semantic segmentation task

As loss function, categorical cross-entropy is used, since the problem of determining the manufacturing processes is modeled as a multi-class classification. For a given face of the 3D CAD model, MaProNet predicts a probability indicating the likelihood that a corresponding technology is used to manufacture the face. The categorical cross-entropy loss (CCE) is calculated as follows:

$$CCE = \frac{1}{M} \sum_{i=1}^M \frac{1}{N} \sum_{j=1}^N \frac{1}{C} \sum_{k=1}^C y_{kji} \cdot \log(\hat{y}_{kji}) \quad (1)$$

where y_{kji} is the true label and \hat{y}_{kji} the predicted probability of the k-th class on the j-th face of the i-th 3D-CAD model.

As metrics, Accuracy, Intersection over Union (IoU), and F1-Score are used. Accuracy measures the overall correctness of the model. It is the ratio of the number of correctly predicted faces to the total number of faces. Due to the nature of the task of predicting manufacturing processes, the different technologies will appear at different rates within

the dataset. Therefore, the dataset will always be imbalanced. A robust metric for imbalanced datasets is the F1-Score, as it considers both precision and recall. Precision is the ratio of correctly predicted positive observations to the total predicted positives. Recall is the ratio of correctly predicted positive observations to all observations in actual class. The F1-Score is the harmonic mean of precision and recall, providing a balance between them. It can be defined as follows:

$$Precision = \frac{TP}{TP + FP} \quad (2)$$

$$Recall = \frac{TP}{TP + FN} \quad (3)$$

$$F1 - Score = 2 \cdot \frac{Precision \cdot Recall}{Precision + Recall} \quad (4)$$

where TP (true positives) is the number of manufacturing processes correctly assigned to the faces of the 3D CAD models, FP (false positives) is the number of manufacturing processes incorrectly assigned to the faces of the 3D CAD models and FN (false negatives) is the number of manufacturing processes incorrectly unassigned.

To further address class imbalance, different weights are assigned to the classes in the loss function. For example, the weight for correct predictions of classes that appear frequently in the dataset is lower, while the weight for predictions of classes that occur rarely is higher. This approach ensures that the model places greater emphasis on underrepresented classes during training. Assigning positive weights in this manner can mitigate the bias towards majority classes, encouraging a more balanced learning process. Therefore, the loss function from (1) needs to be adopted to

$$CCE = \frac{1}{M} \sum_{i=1}^M \frac{1}{N} \sum_{j=1}^N \frac{1}{C} \sum_{k=1}^C w_k \cdot y_{kji} \cdot \log(\hat{y}_{kji}) \quad (5)$$

where w_k is the weight for class k .

At last, IoU, also known as the Jaccard index, is introduced, as it is another typical metric in segmentation tasks. IoU is calculated as the set of overlap between the predicted segmentation and the ground truth, divided by the set of union between the predicted and ground truth. It can be defined as follows:

$$IoU = \frac{1}{M} \sum_{i=1}^M \frac{1}{N} \sum_{j=1}^N \frac{1}{C} \frac{|Y_{ji} \cap \hat{Y}_{ji}|}{|Y_{ji} \cup \hat{Y}_{ji}|} \quad (6)$$

where Y_{ji} is the set of true labels and \hat{Y}_{ji} is the set of predicted labels for the j -th face of the i -th 3D-CAD model.

4. Experimental results and discussion

4.1. Parameter study

In this section, a parameter study is conducted to find a parameter set for MaProNet for further investigations. For the parameter study, the model was trained on a dataset consisting of 60,000 3D CAD models and their corresponding PMI and semantic labels. The dataset was split (75/15/10) for training, validation, and testing respectively. The training was conducted on a NVIDIA Tesla V100 Volta, over 100 epochs and a batch size of 64. As the optimizer, Adam was chosen with a standard choice of parameters. Table 3 summarizes the weights for the different technologies within the loss function.

For example, the weight for a correct positive prediction for the class milling is 1.0, because most of the faces in the dataset are labeled as milling faces. In contrast, the technology reaming appears more rarely in the dataset and therefore a correct positive prediction is linked to a value larger than 1.0. The weights for the different classes, batch size, number of epochs and choice of optimizer were systematically explored in

Table 3

Training weights for the different manufacturing processes.

| Manufacturing Operation | Weight |
|-------------------------|--------|
| Turning | 1.0 |
| Milling | 1.0 |
| Drilling | 1.0 |
| Turning & Grinding | 6.0 |
| Milling & Grinding | 5.0 |
| Drilling & Reaming | 7.0 |

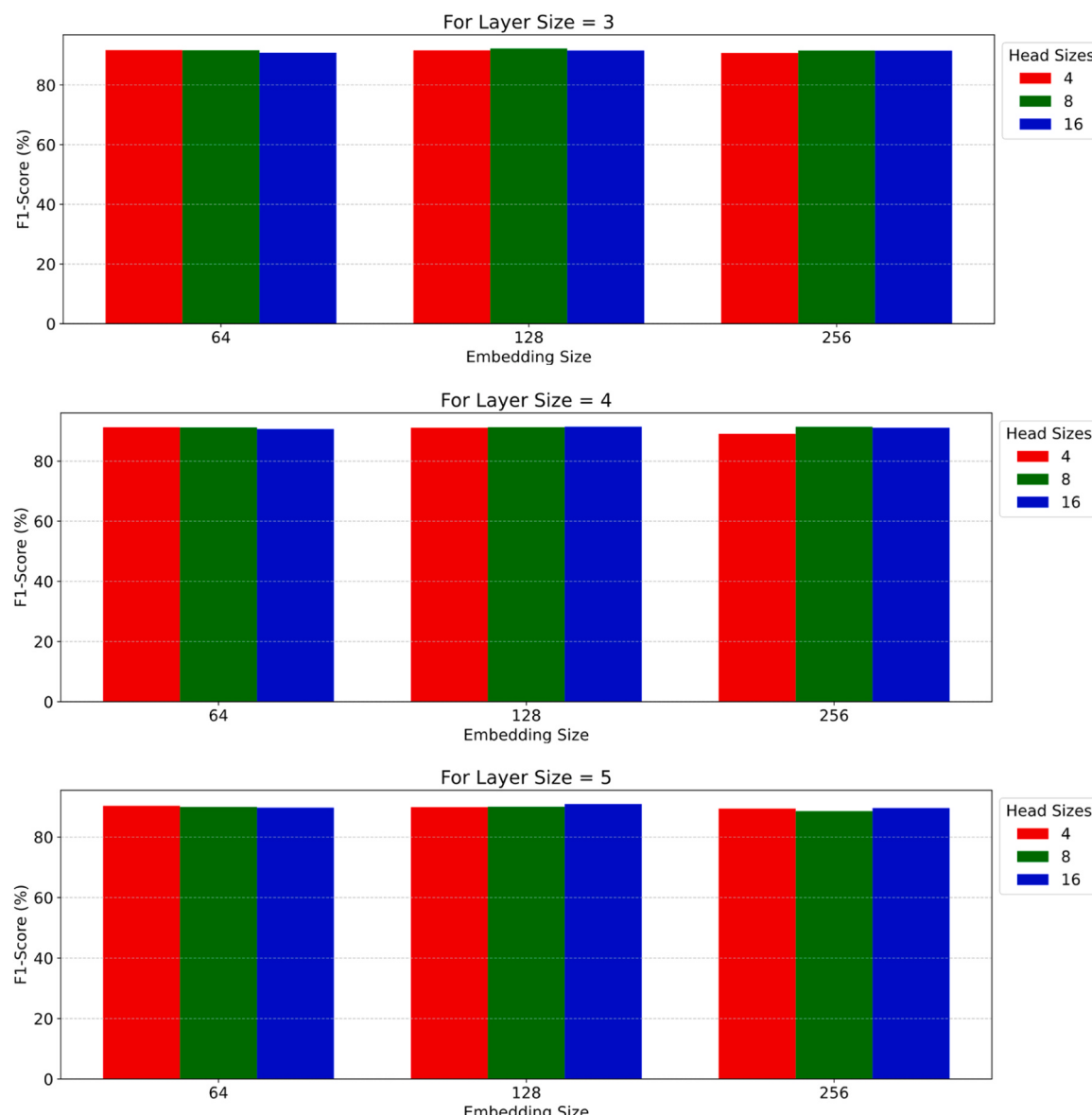
preliminary studies to reduce the combinatorial complexity of the subsequent parameter study to three parameters with a range of three values (27 experiments – full factorial design). Therefore, in the parameter study, the focus is on varying the number of layers, heads, and embedding size. The results can be seen in Fig. 5. A combination of F1-Score, IoU, and Accuracy on test data was used as a measure for the best performing parameter combination.

Overall, the parameter study shows comparable results. Therefore, the choice of parameters does not affect the predictions of the network largely. The results of the different network sizes are within a range of 88.56 % and 92.21 % of F1-Score. Nevertheless, the best model was

found to have an embedding size of 128, 8 attention heads and 3 layer blocks. This model achieved an F1-Score of 92.21 %, an Accuracy of 91.42 % and an IoU of 85.70 %. Consequently, all three metrics suggest a high performance on the test set of the synthetical data. Generally, the following effects can be observed. Increasing the layer size has a small negative effect on the model performance. This effect may be caused by a large increase of trainable parameters with each layer block that is added. Increasing the complexity of the graphs or the number of training data can potentially solve this effect. The number of attention heads has an increasing effect, that diminishes after eight attention heads. As a result, utilizing eight attention heads proves to be the most effective approach for capturing the complexities within the graphs. A similar effect can be found when the size of the embedding is considered. A larger size than 128 will lead to a decrease in performance. This effect may also be caused by a large increase of trainable parameters with each layer that is added, which would require an increase in training size or complexity in graphs.

Fig. 6 summarizes the training results for the best performing model.

Fig. 6 indicates a clear convergence within the training process for both training and validation data. The increase in Accuracy, F1-Score

**Fig. 5.** Results from the parameter study.

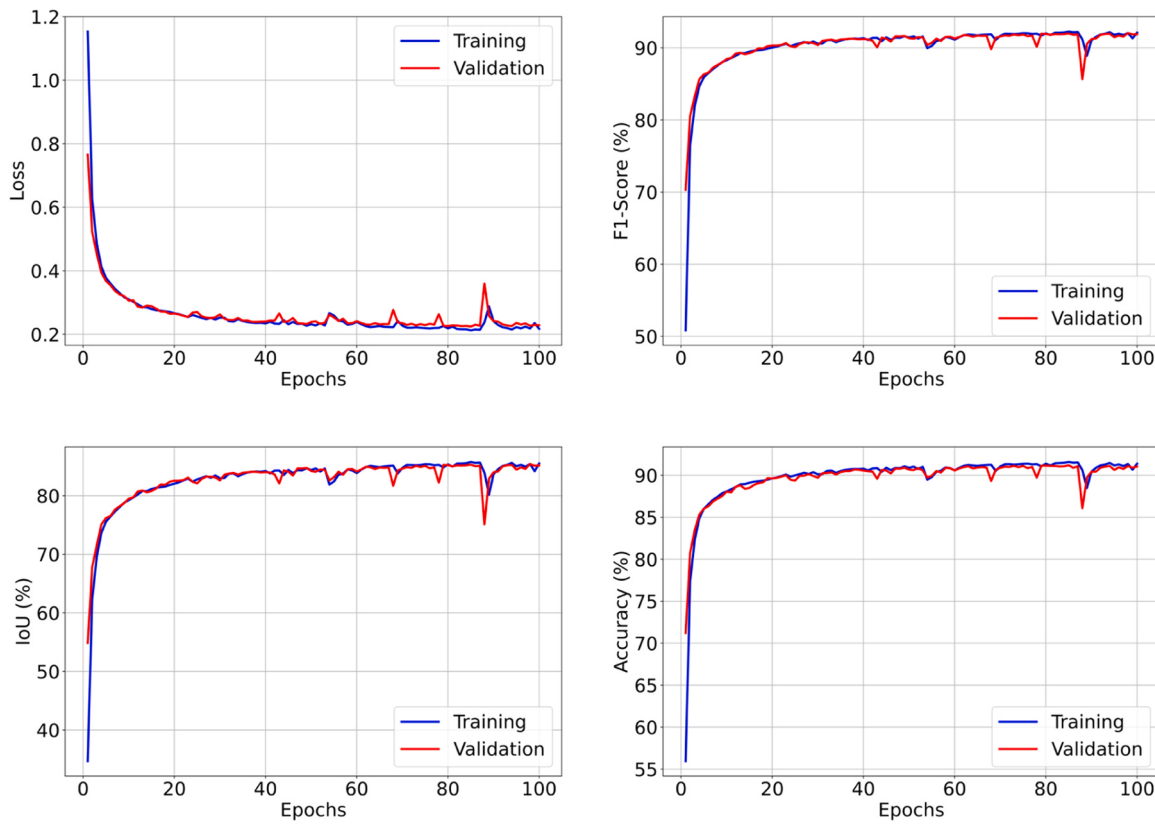


Fig. 6. Training and validation results for the best performing model.

and IoU within the first 40 epochs is larger than for the last 60 epochs. Although the validation loss shows some isolated outliers, overfitting does not appear within the training process. There is no clear increasing trend in the validation loss respectively decreasing trend in validation Accuracy, F1-Score or IoU. A noticeable drop in performance is observed around epoch 90. It is suspected that during the optimization process, the momentum in the optimizer caused the model to escape from a local minimum. However, the impact of this drop on the final results is minimal, as the model's performance recovers and realigns with the previous trend.

4.2. Ablation study

Within this section, an ablation study for MaProNet is conducted. An ablation study is a technique used to evaluate the impact of specific components within a model by systematically removing or modifying them. The goal is to understand the contribution of each component to the overall performance and behavior of the model. In the context of this work, the investigation focuses on the different contributions of the Encoders and their underlying inputs. Therefore, the performance of the model was evaluated by removing the different Encoders (AAG, Mesh and PMI) one by one and measuring the remaining performance and the gap to the model where all possible input encoders are used. Setting the parameters to the ones found in the parameter study (Embedding Size = 128, Head Size = 8, and Layer Size = 3), Fig. 7 summarizes the results of the ablation study.

As can be seen from the results in Fig. 7, removing any input component will lead to a decrease in performance. Therefore, every input for the MaProNet architecture is required for the best performance of the model. The most significant impact can be seen when removing the AAG or Mesh from input for all operations. Mesh and AAG describe similar geometrical and topological attributes whereas the PMI description has a direct effect on the finishing operations. When

considering the rough operations (Milling, Turning, Drilling), AAG and Mesh have almost the same amount of impact, whereas the impact of the PMI is significantly smaller. This effect is caused by the different kinds of geometrical attributes and the neighboring connections of faces that are modeled within the inputs of AAG and Mesh that have a significant influence on the description of the shape of the 3D CAD model. When considering roughing operations that create the geometrical shape of the 3D CAD model, this is of high importance. As can be seen, the definition of PMI has a direct influence on the choice of finishing operations such as grinding and reaming. Therefore, it can be concluded that when the finishing operations are considered the impact of the PMI is highest. Aiming at the explainability of the network, it can therefore be concluded, that MaProNet learned to consider the correct information in the different input types to make the decision on which manufacturing processes to use.

4.3. Comparative Study

Furthermore, the model was tested in a comparative study. The study is conducted to test the performance against the approach of Zhao et al. [4] (MaProVoxel). MaProVoxel was chosen to be compared to MaProNet due to the methodological closeness of the two approaches. Both methods directly select manufacturing processes from the input data, rather than relying on an intermediate feature recognition system. Furthermore, both approaches leverage PMI as part of their modeling process and they have a representation of the 3D structure. While MaProVoxel uses a voxel-based representation, MaProNet utilizes a graph-based representation.

The two approaches are compared using the framework for dataset creation described in this work. Since, the approach MaProVoxel considers only one feature per part, the described framework was adjusted to create 3D CAD models with only one feature. To make the two approaches comparable, MaProNet was adjusted to predict on a global

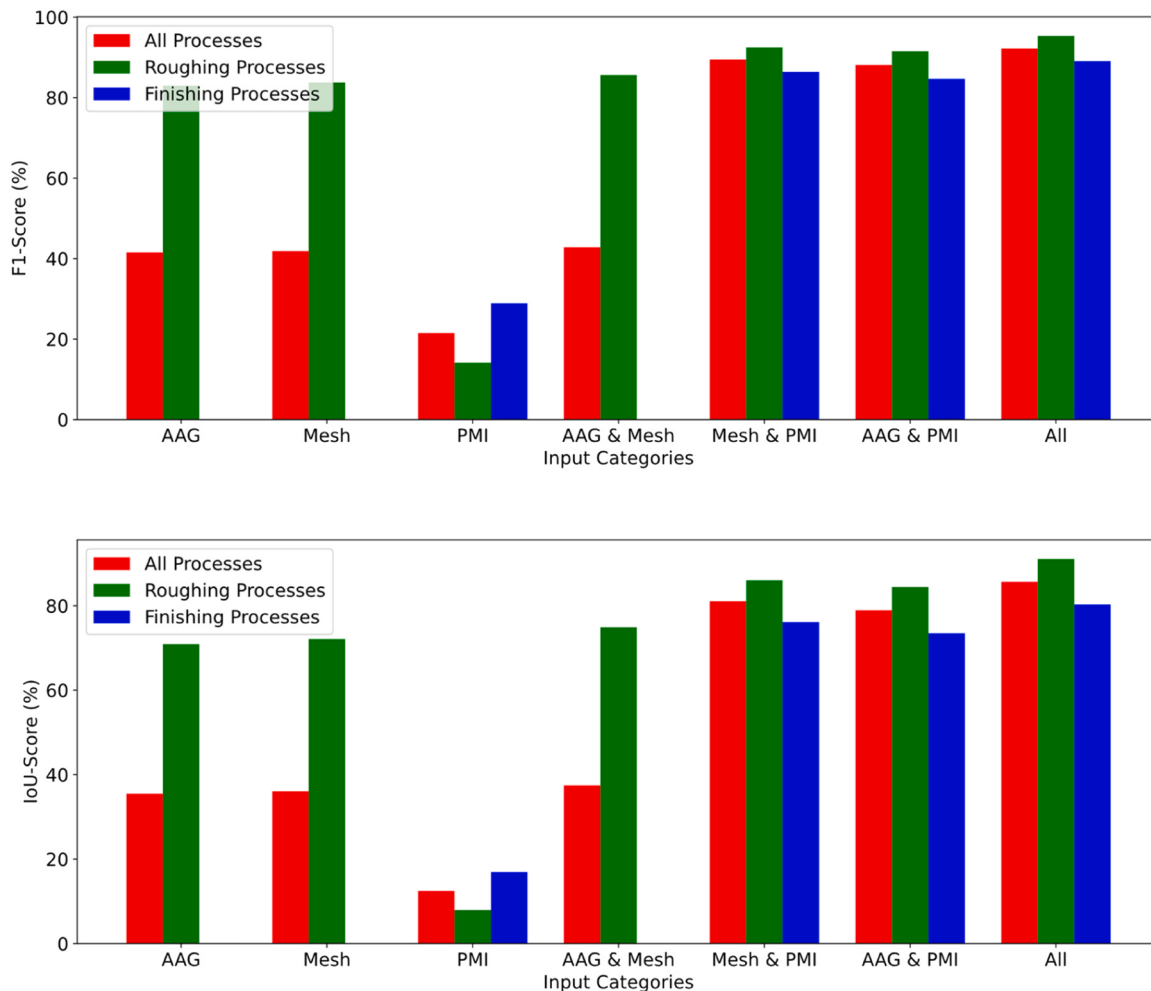


Fig. 7. Results from the ablation study.

scale, by adding an attentional pooling layer to the Decoder to concat the attributes from different faces to the whole 3D CAD model. As the approach from Zhao et al. does not consider all PMI information from this framework, the approach from Zhao et al. was adjusted to also include geometrical tolerances as described in this contribution. The training was conducted on a NVIDIA Tesla V100 Volta, over 100 epochs and a batch size of 64. As the optimizer, Adam was chosen with a standard choice of parameters. The results are summarized in Table 4. The results indicate a better performance of MaProNet compared to MaProVoxel. Furthermore, the computational effort for training MaProNet is lower, due to a decreased training time. Although MaProNet has more parameters to train, the graph structure allows for faster processing compared to the voxel representation.

4.4. Test on industrial data

In this study, MaProNet was evaluated using a set of 30 3D CAD models provided by an industry partner. This assessment aimed to determine the model's predictive accuracy in a real-world industrial setting. The results demonstrate a high degree of accuracy between the model's predictions and the actual labels, underlining the model's

robust performance. Fig. 8 shows ten examples of the industrial dataset.

Quantitatively, the model achieved around 86 % of F1-Score and Accuracy and an IoU of 76 % correct predictions for all the 30 CAD models, which highlights the model's effectiveness and confirms its applicability to industrial data. Overall, the model predicts most of the faces correctly and all of the faces that form one feature are predicted correctly and in the same class. Although for some features in the depicted 3D CAD models, it is predicting several manufacturing technologies for the faces that form one single feature. For example, different faces of the rectangular pocket of part 2 are marked with different technologies. This is the downside of an approach directly predicting the manufacturing processes, since the prediction is done for faces separately, faces from one feature can have several outcomes. Another conclusion that can be seen is the ambiguity of the relationship between features and the manufacturing processes. For part 5 one of the holes is predicted to be milled and ground instead of drilled and reamed which is a permissible choice, but since alternative manufacturing strategies are not taken into account, this prediction is wrong within the metrics. The model is also not able to capture larger patterns, as can be seen from part 7 where one hole is not consistently predicted in alignment with the other predictions. For machining features that are not present in the dataset, as for part 1, the model does not capture the dependency of the faces to each other that form the machining feature and therefore predicts several manufacturing processes for that one feature, but the technologies themselves are permissible. In some cases, round edges (fillets) are marked to be drilled and therefore confused with a hole, as can be seen in part 6.

Table 4

Summary of results from the comparative study.

| Network | F1-Score | Accuracy | IoU | Number of parameters |
|------------|----------|----------|---------|----------------------|
| MaProNet | 92.92 % | 92.81 % | 87.14 % | 3.4 M |
| MaProVoxel | 88.43 % | 88.21 % | 79.52 % | 0.8 M |

| Label | 1 | 2 | 3 | 4 | 5 | |
|------------|------------------------------|------------------------------|------------------------------|------------------------------|------------------------------|--|
| Prediction | | | | | | |
| Evaluation | 32/38 correct predictions | 16/20 correct predictions | 38/42 correct predictions | 15/16 correct predictions | 20/23 correct predictions | |
| Label | 6 | 7 | 8 | 9 | 10 | |
| Prediction | | | | | | |
| Evaluation | 20/23 correct predictions | 20/23 correct predictions | 66/72 correct predictions | 47/51 correct predictions | 23/25 correct predictions | |
| Legend: | | | | | | |

Fig. 8. Results on real industrial data.

5. Summary and outlook

The paper introduced MaProNet, a GAT-based framework tailored for the selection of manufacturing processes on semantically labeled 3D CAD models with PMI. The architecture integrates geometric and topological properties of 3D CAD model faces, leveraging a combination of AAG and Mesh structures. The dataset used to train the model includes 60,000 synthetically generated CAD models, each labeled with specific manufacturing processes on the face level of the model.

The model's performance was evaluated through both synthetic and real-world industrial data, where it achieved high predictive accuracy with over 86 % correctly labeled faces on industrial test data and over 91 % correctly labeled faces on the synthetical data. However, it remains essential for experts to interact with the system to review and

correct its predictions where necessary. Nonetheless, the system provides significant support for planners by achieving the described accuracy. This high level of precision reduces the time and effort required for planning the required manufacturing processes.

However, there are still some limitations. While the proposed approach is formulated as a multi-class classification problem, it does not explicitly model alternative process plans. Integrating such alternatives could enhance flexibility for downstream tasks such as scheduling and resource allocation. Another limitation of the current approach is that it considers only the specified manufacturing processes. However, extending the methodology to incorporate additional processes or a more detailed differentiation of e.g. various milling strategies would require the definition of additional classes to represent new processes appropriately. Furthermore, the synthetic data would require

refinement with more complex rules to ensure consistency and accuracy in representing the expanded process space. Therefore, future work could focus on systematically integrating a broader range of manufacturing processes and exploring the feasibility of utilizing industry data for improved model generalization, potentially leveraging transfer learning. Additionally, this study focuses on PMI that are directly associated with individual faces. Future research could extend this approach by incorporating indirect PMI, which defines tolerances between faces and are typically linked via datums—for example, parallelism or positional tolerances. Since these PMI also influence process selection, their inclusion could further refine the predictive capabilities of the model.

CRediT authorship contribution statement

Hussong Marco: Writing – original draft, Visualization, Validation, Software, Methodology, Conceptualization. **Klar Matthias:** Writing –

review & editing. **Ruediger-Flore Patrick:** Writing – original draft. **Aurich Jan C.:** Writing – review & editing, Project administration. **Kloft Marius:** Writing – review & editing, Project administration.

Declaration of Competing Interest

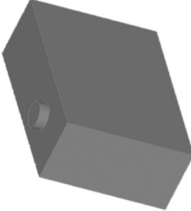
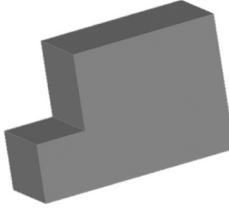
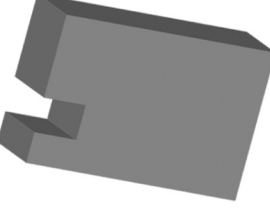
The authors declare that they have no known competing financial interests or personal relationships that could have appeared to influence the work reported in this paper.

Acknowledgment

The research was founded by the Ministerium für Wirtschaft, Verkehr, Landwirtschaft und Weinbau from the State Rhineland-Palatinate in Germany within the project „KI4KMU-RLP - Erforschung und Transfer nachhaltiger Kl-Innovationen für produzierende KMU in Rheinland-Pfalz“.

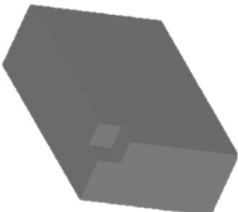
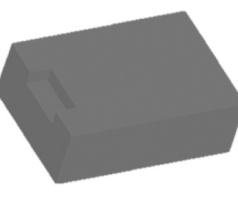
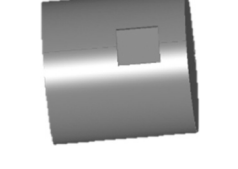
Appendix

Table 5
Overview of the modeled part features and their parameters

| Feature type | Feature illustration | Parameter range (x% of side length) | Possible PMI |
|--------------|---|---|---|
| Cuboid Boss |  | Length: 20 %–50 % Width: 20 %–50 % Depth: 5 %–10 % | Straightness Flatness |
| Round Boss |  | Radius: 10 %–20 % Depth: 5 %–10 % | Circularity Cylindricity Flatness Straightness |
| Through Step |  | Length: 10 %–90 % Depth: 10 %–66 % | Flatness Straightness |
| Through Slot |  | Width: 10 %–50 % Depth: 10 %–66 % | Flatness Straightness |

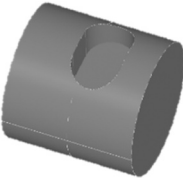
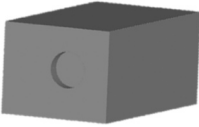
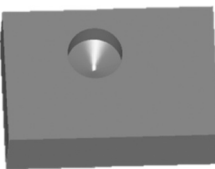
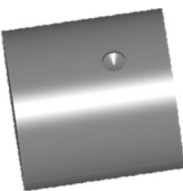
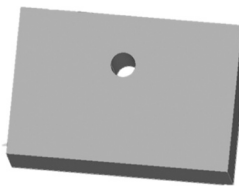
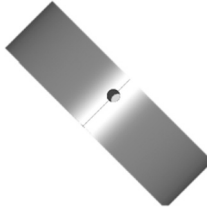
(continued on next page)

Table 5 (continued)

| | | | |
|---------------------|---|--|-----------------------------|
| |  | Width: 10 %–50 % Depth: 1 %–10 % | Flatness Straightness |
| Blind Step |  | Length: 1 %–80 % Width: 1 %–80 % Depth: 10 %–66 % | Flatness Straightness |
| Blind Slot |  | Width: 10 %–50 % Depth: 10 %–66 % | Flatness Straightness |
| Cylinder Step |  | Radius: 50 %–90 % Length: 5 %–50 % | Circularity Cylindricity |
| Rectangular Pocket |  | Length: 10 %–33 % Width: 10 %–33 % Depth: 10 %–25 % | Flatness Straightness |
| |  | Length: 10 %–33 % Width: 10 %–33 % Depth: 10 %–25 % | Flatness Straightness |
| Circular End Pocket |  | Radius: 5 %–10 % Length: 10 %–20 % Depth: 10 %–25 % | Flatness Straightness |

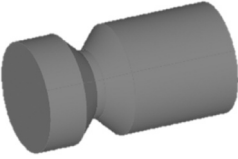
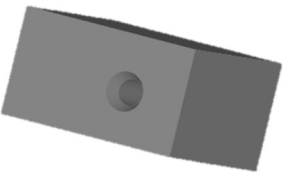
(continued on next page)

Table 5 (continued)

| | | | |
|--------------------|---|--|-----------------------------|
| |  | Radius: 5 %–10 % Length: 10 %–20 % Depth: 10 %–25 % | Flatness Straightness |
| Milled Blind Hole |  | Depth: 10 %–80 % Radius: 2.5 %–25 % | Circularity Cylindricity |
| |  | Depth: 10 %–80 % Radius: 2.5 %–25 % | Circularity Cylindricity |
| Drilled Blind Hole |  | Depth: 10 %–80 % Radius: 2.5 %–25 % | Circularity Cylindricity |
| |  | Depth: 10 %–80 % Radius: 2.5 %–25 % | Circularity Cylindricity |
| Through Hole |  | Radius: 1 %–25 % | Circularity Cylindricity |
| |  | Radius: 1 %–25 % | Circularity Cylindricity |
| Chamfer |  | Length: 0.1–2 | / |

(continued on next page)

Table 5 (continued)

| | | | |
|---------------------|---|--|-----------------------------|
| |  | Length: 0.1–2 | / |
| Fillet |  | Radius: 0.5–2 | / |
| |  | Radius: 0.5–2 | / |
| Groove |  | Width: 1–3 Depth: 10 %–50 % | Circularity Cylindricity |
| Belt Step |  | Depth: 10 %–50 % Length: 3–5 | Circularity Cylindricity |
| Taper |  | Depth: 10 %–50 % Length: 3 %–5 % | Circularity Cylindricity |
| Countersink Hole |  | Radius 2,5 %–12,5 % Depth Sink: 18 %–33 % Radius Sink: 120 %–180 % Radius | Circularity Cylindricity |
| |  | Radius 5 %–12,5 % Depth Bore: 12,5 %–25 % Radius Bore: 120 %–200 % Radius | Circularity Cylindricity |

(continued on next page)

Table 5 (continued)

| | | | |
|---------------------|---|--|-----------------------------|
| Counterbore Hole |  | Radius 2,5 %–12,5 % Depth Bore: 12,5 %–25 % Radius Bore: 120 %–200 % Radius | Circularity Cylindricity |
| |  | Radius 5 %–12,5 % Depth Bore: 12,5 %–25 % Radius Bore: 120 %–200 % Radius | Circularity Cylindricity |

Table 6

Results from the parameter study

| Embedding size | Head size | Layer size | F1-Score | Acc | IoU |
|----------------|-----------|------------|----------------|----------------|----------------|
| 64 | 4 | 3 | 91.69 % | 90.62 % | 84.84 % |
| 64 | 4 | 4 | 9127 % | 90.78 % | 84.14 % |
| 64 | 4 | 5 | 90.33 % | 90.21 % | 82.57 % |
| 64 | 8 | 3 | 91.60 % | 91.12 % | 84.69 % |
| 64 | 8 | 4 | 91.22 % | 90.64 % | 84.05 % |
| 64 | 8 | 5 | 89.97 % | 89.89 % | 81.99 % |
| 64 | 16 | 3 | 90.81 % | 90.65 % | 83.40 % |
| 64 | 16 | 4 | 90.67 % | 90.52 % | 83.16 % |
| 64 | 16 | 5 | 89.70 % | 89.66 % | 81.60 % |
| 128 | 4 | 3 | 91.58 % | 91.00 % | 84.64 % |
| 128 | 4 | 4 | 91.11 % | 90.33 % | 83.84 % |
| 128 | 4 | 5 | 89.90 % | 89.40 % | 81.85 % |
| 128 | 8 | 3 | 92.21 % | 91.42 % | 85.70 % |
| 128 | 8 | 4 | 91.28 % | 90.78 % | 84.13 % |
| 128 | 8 | 5 | 90.04 % | 89.73 % | 82.09 % |
| 128 | 16 | 3 | 91.53 % | 91.24 % | 84.56 % |
| 128 | 16 | 4 | 91.44 % | 91.11 % | 84.44 % |
| 128 | 16 | 5 | 90.94 % | 90.57 % | 83.56 % |
| 256 | 4 | 3 | 90.73 % | 89.85 % | 83.22 % |
| 256 | 4 | 4 | 89.06 % | 88.00 % | 80.46 % |
| 256 | 4 | 5 | 89.42 % | 88.33 % | 80.97 % |
| 256 | 8 | 3 | 91.52 % | 90.57 % | 84.53 % |
| 256 | 8 | 4 | 91.41 % | 90.62 % | 84.33 % |
| 256 | 8 | 5 | 88.56 % | 88.33 % | 79.67 % |
| 256 | 16 | 3 | 91.49 % | 90.56 % | 84.48 % |
| 256 | 16 | 4 | 91.10 % | 90.02 % | 83.82 % |
| 256 | 16 | 5 | 89.59 % | 89.38 % | 81.35 % |

References

- [1] Soori M, Asmael M. Classification of research and applications of the computer aided process planning in manufacturing systems. *Indep J Manag Prod* 2021;12(5): 1250–81. <https://doi.org/10.14807/ijmp.v12i5.1397>.
- [2] Lu Y, Xu X, Wang L. Smart manufacturing process and system automation – A critical review of the standards and envisioned scenarios. *J Manuf Syst* 2020;56: 312–25. <https://doi.org/10.1016/j.jmansys.2020.06.010>.
- [3] Trstenjak M, Cosic P. Process planning in industry 4.0 environment. *Procedia Manuf* 2017;11:1744–50. <https://doi.org/10.1016/j.promfg.2017.07.303>.
- [4] Zhao C, Melkote SN. Learning the manufacturing capabilities of machining and finishing processes using a deep neural network model. *J Intell Manuf* 2024;35: 1845–65. <https://doi.org/10.1007/s10845-023-02134-z>.
- [5] Wang Z, Yan X, Bjorni J, Dinar M, Melkote S, Rosen D. Manufacturing process selection based on similarity search: incorporating non-shape information in shape descriptor comparison. *J Intell Manuf* 2024. <https://doi.org/10.1007/s10845-024-02368-5>.
- [6] Gu P, Zhang Y. Operation sequencing in an automated process planning system. *J Intell Manuf* 1993;4(3):219–32. <https://doi.org/10.1007/BF00123966>.
- [7] Eum K, Kang M, Kim G, Park MW, Kim JK. Ontology-based modeling of process selection knowledge for machining feature. *Int J Precis Eng Manuf* 2013;14(10): 1719–26. <https://doi.org/10.1007/s12541-013-0231-7>.
- [8] Deja M, Siemiatkowski MS. Feature-based generation of machining process plans for optimised parts manufacture. *J Intell Manuf* 2013;24(4):831–46. <https://doi.org/10.1007/s10845-012-0633-x>.
- [9] Zhu J, Muto S, Tanaka T, Saito Y. Development of automatic machining process deciding system based on 3D-model. Proceedings of international conference on leading edge manufacturing in 21st century. LEM21 2013;2013;7:123–8. <https://doi.org/10.1299/jsmelem.2013.7.123>.
- [10] Sormaz D, Gouveia R, Sarkar A. Rule based process selection of milling processes based on gd&t requirements. *J Prod Eng* 2018;21(2):19–26. <https://doi.org/10.24867/JPE-2018-02-019>.
- [11] Sormaz D, Sarkar A. SIMPM – Upper-level ontology for manufacturing process plan network generation. *Robot Comput-Integr Manuf* 2019;55:183–98. <https://doi.org/10.1016/j.rcim.2018.04.002>.
- [12] Sarkar A, Sormaz D. Ontology model for process level capabilities of manufacturing resources. *Procedia Manuf* 2019;39:1889–98. <https://doi.org/10.1016/j.promfg.2020.01.244>.

- [13] Ahmad N, Haque A. Artificial neural networks based process selection for cylindrical surface machining. *Proc Int Conf Manuf* 2002.
- [14] Yahia NB, Fnaiech F, Abid S, Sassi BH. Manufacturing process planning application using artificial neural networks. *IEEE Int Conf Syst, Man Cybern* 2002;5. <https://doi.org/10.1109/ICSMC.2002.1176443>.
- [15] Deb S, Para-Castillo R, Ghosh K. An integrated and intelligent computer-aided process planning methodology for machined rotationally symmetrical parts. *Int J Adv Manuf Syst* 2011;13(1):1–26.
- [16] Gizaw M, Rani M, Yusof Y. Turn-mill process plan and intelligence machining operations selection on STEP. *Asian J Sci Res* 2013;6(2):346–52.
- [17] Abdulghafour A, Neama Z. Integrated of machining operation sequences and cutting tools selection based artificial neural network for rotational parts. *Int J Sci: Basic Appl Res* 2018;38(1):170–88.
- [18] Natarajan KK, Gokulachandran J. Artificial neural network based machining operation selection for prismatic components. *Int J Adv Sci, Eng Inf Technol* 2020; 10(2):618. <https://doi.org/10.18517/ijaseit.10.2.8646>.
- [19] Wang Z, Zhang S, Zhang H, Zhang Y, Liang J, Huang R, et al. Machining feature process route planning based on a graph convolutional neural network. *Adv Eng Inform* 2024;59. <https://doi.org/10.1016/j.aei.2023.102249>.
- [20] Zhao C, Dinar M, Melkote SN. Deep learning and sequence mining for manufacturing process and sequence selection. *Int J Prod Res* 2024;62(14):1–22. <https://doi.org/10.1080/00207543.2023.2290700>.
- [21] Shi Y, Zhang Y, Xia K, Harik R. A critical review of feature recognition techniques. *Comput-Aided Des Appl* 2020;17(5):861–99. <https://doi.org/10.14733/cadaps.2020.861-899>.
- [22] Zhang Z, Jaiswal P, Rai R. FeatureNet: machining feature recognition based on 3D convolution neural network. *Comput-Aided Des* 2018;101:12–22. <https://doi.org/10.1016/j.cad.2018.03.006>.
- [23] Ma Y, Zhang Y, Luo X. Automatic recognition of machining features based on point cloud data using convolution neural Networks. *Proc 2019 Int Conf Artif Intell Comput Sci* 2019;229–35. <https://doi.org/10.1145/3349341.3349407>.
- [24] Shi P, Qi Q, Qin Y, Scott PJ, Jiang X. A novel learning-based feature recognition method using multiple sectional view representation. *J Intell Manuf* 2020;31(5): 1291–309. <https://doi.org/10.1007/s10845-020-01533-w>.
- [25] Ning F, Shi Y, Cai M, Xu W. Part machining feature recognition based on a deep learning method. *J Intell Manuf* 2021;34(2):809–21. <https://doi.org/10.1007/s10845-021-01827-7>.
- [26] Yeo C, Kim BC, Cheon S, Lee J, Mun D. Machining feature recognition based on deep neural networks to support tight integration with 3D CAD systems. *Sci Rep* 2021;11(1). <https://doi.org/10.1038/s41598-021-01313-3>.
- [27] Colligan AR, Robinson TT, Nolan DC, Hua Y, Cao W. Hierarchical CADNet: learning from b-reps for machining feature recognition. *Comput-Aided Des* 2022;147: 103226. <https://doi.org/10.1016/j.cad.2022.103226>.
- [28] Lee J, Lee H, Mun D. 3D convolutional neural network for machining feature recognition with gradient-based visual explanations from 3D CAD models. *Sci Rep* 2022;12(1):14864. <https://doi.org/10.1038/s41598-022-19212-6>.
- [29] Yao X, Di Wang, Yu T, Luan C, Fu J. A machining feature recognition approach based on hierarchical neural network for multi-feature point cloud models. *J Intell Manuf* 2022;34:2599–610. <https://doi.org/10.1007/s10845-022-01939-8>.
- [30] Zhang H, Zhang S, Zhang Y, Liang J, Wang Z. Machining feature recognition based on a novel multi-task deep learning network. *Robot Comput-Integr Manuf* 2022;77: 102369. <https://doi.org/10.1016/j.rcim.2022.102369>.
- [31] Jia J-L, Zhang S-W, Cao Y-R, Qi X-L, WeZhu. Machining feature recognition method based on improved mesh neural network. *Iran J Sci Technol, Trans Mech Eng* 2023;47(4):2045–58. <https://doi.org/10.1007/s40997-023-00610-8>.
- [32] Lee J, Yeo C, Cheon S-U, Park JH, Mun D. BRepGAT: graph neural network to segment machining feature faces in a B-rep model. *J Comput Des Eng* 2023;10(6): 2384–400. <https://doi.org/10.1093/jcde/qwad106>.
- [33] Wang P, Yang W-A, You Y. A hybrid learning framework for manufacturing feature recognition using graph neural networks. *J Manuf Process* 2023;85:387–404. <https://doi.org/10.1016/j.jmapro.2022.10.075>.
- [34] Wu H, Lei R, Huang P, Peng Y. A semi-supervised learning framework for machining feature recognition on small labeled sample. *Appl Sci* 2023;13(5):3181. <https://doi.org/10.3390/app13053181>.
- [35] Zhang S, Guan Z, Jiang H, Wang X, Tan P. BrepMFR: enhancing machining feature recognition in B-rep models through deep learning and domain adaptation. *Comput Aided Geom Des* 2024;111:102318. <https://doi.org/10.1016/j.cagd.2024.102318>.
- [36] Wu H, Lei R, Peng Y, Gao L. AAGNet: a graph neural network towards multi-task machining feature recognition. *Robot Comput-Integr Manuf* 2024;86:102661. <https://doi.org/10.1016/j.rcim.2023.102661>.
- [37] Peddireddy D, Fu X, Shankar A, Wang H, Joung BG, Aggarwal V, et al. Identifying manufacturability and machining processes using deep 3D convolutional networks. *J Manuf Process* 2021;64:1336–48. <https://doi.org/10.1016/j.jmapro.2021.02.034>.
- [38] Fu X, Peddireddy D, Aggarwal V, Jun MB-G. Improved dixel representation: A 3-D CNN geometry descriptor for manufacturing CAD. *IEEE Trans Ind Inform* 2022;18(9):5882–92. <https://doi.org/10.1109/TII.2021.3136167>.
- [39] Wang Z, Rosen D. Manufacturing process classification based on heat kernel signature and convolutional neural networks. *J Intell Manuf* 2022;34:3389–411. <https://doi.org/10.1007/s10845-022-02009-9>.
- [40] Yan X, Wang Z, Bjorni J, Zhao C, Dinar M, Rosen D, et al. Process-aware part retrieval for cyber manufacturing using unsupervised deep learning. *CIRP Ann* 2023;72(1):397–400. <https://doi.org/10.1016/j.cirp.2023.03.020>.
- [41] Yan X, Melkote S. Automated manufacturability analysis and machining process selection using deep generative model and Siamese neural networks. *J Manuf Syst* 2023;67:57–67. <https://doi.org/10.1016/j.jmsy.2023.01.006>.
- [42] Yan X, Williams R, Arvanitis E, Melkote S. Deep learning-based semantic segmentation of machinable volumes for cyber manufacturing service. *J Manuf Syst* 2024;72:16–25. <https://doi.org/10.1016/j.jmsy.2023.11.005>.
- [43] The American Society of Mechanical Engineers. Surface texture (surface roughness, waviness, and lay) an international standard. ASME(B46.1-1019). New York, NY: The American Society of Mechanical Engineers; 2020.